European Journal of Pharmacology 954 (2023) 175861

Contents lists available at ScienceDirect

European Journal of Pharmacology

journal homepage: www.elsevier.com/locate/ejphar

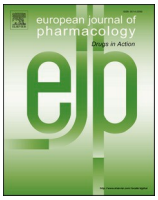

A specific RAGE-binding peptide inhibits triple negative breast cancer growth through blocking of Erk1/2/NF-κB pathway

Xiaoyong Dai [a,1], Yibo Hou [a,1], Ting Deng [a,1], Gaoyang Lin [a], Yuanxiong Cao [a], Guiyuan Yu [b], Wei Wei [c], Qing Zheng [d], Laiqiang Huang [a,*], Shaohua Ma [a,**]

[a] Institute of Biopharmaceutical and Health Engineering, Shenzhen Key Laboratory of Gene and Antibody Therapy, State Key Laboratory of Chemical Oncogenomics, Shenzhen International Graduate School, Tsinghua University, Shenzhen, Guangdong, 518055, China
[b] Shenzhen Maternal and Child Health Hospital Affiliated to Southern Medical University, Shenzhen, Guangdong, China
[c] The Department of Breast and Thyroid Surgery, Peking University Shenzhen Hospital, Shenzhen, Guangdong, 518036, China
[d] College of Pharmacy, Jinan University, 510632 Guangzhou, Guangdong, People's Republic of China

ARTICLE INFO

Keywords:
TNBC
RAGE
RP7
HMGB1
NF-κB pathway
Apoptosis

ABSTRACT

Triple-negative breast cancer (TNBC) is an aggressive cancer that poses a significant threat to women's health. Unfortunately, the lack of clinical targets leads the poor clinical outcomes in TNBC. Many cancers demonstrate overexpression of receptor for advanced glycation end products (RAGE), which can contribute to cancer progression. Despite the potential therapeutic value of blocking RAGE for TNBC treatment, effective peptide drugs have yet to be developed. In our study, we observed that RAGE was highly expressed in TNBC and was associated with poor disease progression. We subsequently investigated the antitumor effects and underlying mechanisms of the RAGE antagonist peptide RP7 in both *in vitro* and *in vivo* models of TNBC. Our study revealed that RP7 selectively binds to RAGE-overexpressing TNBC cell lines, including MDA-MB-231 and BT549, and significantly inhibits cell viability, migration, and invasion in both cell lines. Furthermore, RP7-treatment suppressed tumor growth in TNBC xenograft mouse models without inducing detectable toxicity in normal tissues. Mechanistically, RP7 was found to inhibit the phosphorylation of ERK1/2, IKKα/β, IKBα, and p65 to block the NF-κB pathway, prevent the entry of p65 into the nucleus, decrease the protein expression of Bcl-2 and HMGB1, and promote the release of cytochrome C from the mitochondria into the cytoplasm. These effects were observed to activate apoptosis and inhibit epithelial-mesenchymal transition (EMT) in TNBC cells. This study highlights RAGE as a candidate therapeutic target for TNBC treatment and suggests that the RAGE antagonist peptide RP7 is a promising anticancer drug for TNBC.

1. Introduction

Triple-negative breast cancer (TNBC) is typically characterized by negative expression of estrogen (ER), progesterone (PR), and human epidermal growth factor receptor-2 (HER2) (Boyle, 2012; Wolff et al., 2013). Between 2012 and 2016, TNBC accounted for 12% of breast cancer diagnoses in the United States and was associated with a 5-year survival rate 8–16% lower than other types of breast cancer (Howard and Olopade, 2021). TNBC is known to be more aggressive than other types of breast cancer, with a 46% probability of metastasis to sites such as the brain and visceral organs (Yin et al., 2020). Therefore, patients with TNBC often experience relapse within 19–40 months after initial treatment, and have a high mortality rate of 75% within 3 months after recurrence (Gluz et al., 2009; Lin et al., 2008).

The receptor of advanced glycation end products (RAGE) was primarily recognized from non-enzymatic glycation that forms during hyperglycemia as a result of poor diabetic control (Palanissami and Paul, 2018). Further investigation have found that RAGE is a multiligand receptor for high mobility group box 1 (HMGB1) and the S100 calcium-binding protein B (S100B) (Ahmad et al., 2018; Hudson and Lippman, 2018). The RAGE-ligand axis has been implicated in various physiological processes, including homeostasis, development, inflammation, as well as in several disease states (Wautier et al., 1996; Yan

* Corresponding author.
** Corresponding author.
E-mail addresses: huanglq@tsinghua.edu.cn (L. Huang), ma.shaohua@sz.tsinghua.edu.cn (S. Ma).
[1] These authors contributed equally to this work: Xiaoyong Dai, Yibo Hou and Ting Deng.

https://doi.org/10.1016/j.ejphar.2023.175861
Received 9 January 2023; Received in revised form 12 June 2023; Accepted 15 June 2023
Available online 26 June 2023
0014-2999/© 2023 The Authors. Published by Elsevier B.V. This is an open access article under the CC BY-NC-ND license (http://creativecommons.org/licenses/by-nc-nd/4.0/).

Abbreviation

TNBC	the triple-negative breast cancer
RAGE	the receptor of advanced glycation end products
HMGB1	high mobility group box 1
ER	estrogen
PR	progesterone
HER2	human epidermal growth factor receptor-2
S100B	S100 calcium-binding protein B
PRRs	pattern recognition receptors
TNFR	TNF receptor
MMP	Matrix metalloproteinases
EMT	epithelial-mesenchymal transition
DMEM	Dulbecco's Modified Eagle Medium
FBS	fetal bovine serum
MTT	3-(4,5-Dimethylthiazol-2-yl)-2,5-diphenyltetrazolium bromide
DMSO	dimethyl sulfoxide
DAPI	2-(4-Amidinophenyl)-6-indolecarbamidine dihydrochloride
RIPA	radioimmunoprecipitation assay
EdU	5-Ethynyl-2′-deoxyuridine
TUNEL	Terminal deoxynucleotidyl transferase dUTP nick end labeling
HE	hematoxylin-eosin
IHC	immunohistochemistry
ALT	aminotransferase
AST	aspartate aminotransferase
ALP	alkaline phosphatase
TG	triglyceride (TG)

et al., 1996). Elevated expression levels of RAGE and its ligands have been linked to metastasis and poor prognosis in various types of tumors, such as prostate, gastric, breast, and colon cancer (Kuniyasu et al., 2002; Ishiguro et al., 2005). Kwak et al. demonstrated that therapeutic inhibition of RAGE-ligand signaling can impair breast cancer cell invasion and metastasis, suggesting that it may represent a novel and potent approach to treating invasive and metastatic breast cancer (Kwak et al., 2017).

NF-κB is a member of the inducible transcription factor family that plays a crucial role in controlling and regulating immune and inflammatory responses (Oeckinghaus and Ghosh, 2009). The NF-κB mainly involves in canonical and noncanonical (or alternative) pathways (Moynagh, 2005; Vallabhapurapu and Karin, 2009). The canonical NF-κB pathway can be activated by responding to various stimuli, such as ligands of cytokine receptors, pattern recognition receptors (PRRs), members of the TNF receptor (TNFR) superfamily, as well as the T-cell receptor (TCR) and B-cell receptor (Zhang and Sun, 2015). Whereas, the noncanonical (or alternative) pathways selectively responds to specific stimuli, including ligands of a subset of TNFR superfamily members such as LTβR, BAFFR, CD40 and RANK (Sun, 2011). It has been well investigated that RAGE signal activated intracellular cell signaling including NF-κB, leading to inflammation (Wang et al., 2020). The RAGE/NF-κB signaling pathway plays a crucial role in promoting tumor growth by maintaining inflammatory signaling in pancreatic ductal adenocarcinoma (Azizan et al., 2017), prostate cancer (Somensi et al., 2017), lung cancer (Somensi et al., 2017). A recent study has investigated the suppression of HMGB1/RAGE and its effect on cancer cell apoptosis in an Bcl-2-regulated manner, as well as its role in reducing the phosphorylation of NF-κB in acute leukemia (Lai et al., 2021). Therefore, RAGE may become a potential target in cancer therapy.

In our previously study, eight novel RAGE binding peptides with high binding affinity to RAGE were screening by phage display technology (Cai et al., 2016). In this study, we observed that RP7 peptide exhibited the highest cytotoxic activity against TNBC cells compared to seven other peptides. Therefore, we selected RP7 for further investigation to explore its antitumor effects and underlying mechanism in TNBC treatment, as indicated by the MTT results.

2. Materials and methods

2.1. Cell culture and cell lines

MCF-7, BT549, MBA-MD-231, SKBR3, T47D, 293 T, MCF10A and HCC1937 cell lines were all purchased from the Chinese Academy of Sciences Cell Bank (Shanghai, China). All cells were cultured in Gibco Dulbecco's Modified Eagle Medium (DMEM, Gibco, C11995500BT) supplemented with 10% FBS (QmSuero, mu001SR), 100 μg/ml streptomycin, and 100 U/mL penicillin (TRANS, FG101-01). Cells were incubated in a humidified incubator at 37 °C and 5% CO_2. Cells were passaged at 80% confluence using trypsin-EDTA (TRANS, FG301-01) every 2–4 days. Prior to use in experiments, cells were checked for morphology and viability using a light microscope.

2.2. Cell viability assay

The MTT assay was used to measure cellular metabolic activity as an indicator of cell viability of BT549 and MBA-MD-231. Cells were seeded into 96-well plates at 7.5×10^3 cells per well and allowed to adhere for 24 h in an incubator. After 24 h, gradient concentrations of peptide RP7 (100, 50, 25, 12.5, 6.25, 3.125 μM) were added into planking cells for 24, 48, and 72 h. After treatment, fresh medium supplemented with 5 mg/ml of MTT (Aladdin, M158055) were added to obtain formazan. Furthermore, the MTT-containing medium was then removed and replaced with 150 μl of pure DMSO (Sigma-Aldrich, 200-664-3) to solubilize the formazan crystals formed by viable cells. The absorbance at 570 nm was measured using EnSight Multimode Plate Reader (PerkinElmer, Singapore).

2.3. Immunofluorescence

Immunofluorescence was performed to assess the localization of RAGE in TNBC cells. Cells were seeded on confocal dishes and allowed to adhere for 24 h until 70% confluency. Cells were then fixed with 4% paraformaldehyde (Servicebio, G1101) for 20 min at room temperature and permeabilized with 0.1% Triton X-100 (Sangon Biotech, F724BA0019) in phosphate-buffered saline (PBS, pH = 7.4) for 10 min. Non-specific binding was blocked with 5% bovine serum albumin (BSA) in PBS for 1 h at room temperature. Cells were then incubated with a primary antibody against RAGE (1:100 dilution) (ABclonal Technology Co.,Ltd., A23422) overnight at 4 °C. After washing with PBS, cells were then incubated with 10 μM peptide-FITC for 1 h at room temperature. After washing with PBS, cells were incubated with a secondary antibody conjugated to Alexa Fluor 488 (1:500 dilution) (CST, 4412 S) for 1 h at room temperature. Nuclei were counterstained with 4',6-diamidino-2-phenylindole (DAPI) (1:1000 dilution) (Sigma-Aldrich, D9542) for 5 min. All images were captured by super-resolution microscopy (Nikon, USA).

2.4. Cell apoptosis analysis

The TNBC cells (4×10^5) were seeded into 6-well plates and allowed to adhere for 24 h. Then, cells were treated with RP7 (50 μM, 25 μM) for 48 h. After treatment, cells were harvested and washed with cold PBS. Cells were digested with 0.05% Trypsin (no EDTA), cells were then

resuspended in 1 × binding buffer and stained with Annexin V-FITC/PI Kit (4 A Biotech, FXP018-100) for apoptosis detection according to the manufacturer's protocol. Apoptosis results were analyzed by FlowJo Software (Beckman, USA).

2.5. Cell proliferation by EdU

The cell proliferation was detected using the incorporation of 5-Ethynyl-2′-deoxyuridine (EdU) with the EdU Cell Proliferation Assay Kit (Ribobio, C10310-3). TNBC cells were seeded in 6-well plates at a density of 4×10^5 cells per well and allowed to adhere for 24 h. Further, cells were treated with RP7 (50 μM, 25 μM) for 24 h. During the last 2 h of treatment, cells were incubated with 50 μM EdU. The permeabilization and EdU staining were also performed according to the manufacturer's protocol. The cell nuclei were stained with Hoechst at a concentration of 1 μg/mL for 30 min. The proportion of cells that incorporated EdU was determined using the fluorescence microscopy.

2.6. Western blot

MB-MDA-231 and BT549 cells treated RP7 (50 μM, 25 μM) were collected and lysed with RIPA Lysis Buffer (MedChemExpress, HY-K1001), and then centrifuged at 14,000 rpm for 30 min at 4 °C. The supernatant was collected, and total protein concentration was determined with the Pierce BCA Protein Assay Kit (Thermo Scientific, A53225). The 10% SDS-PAGE was prepared in advance with the PAGE Gel Fast Preparation Kit (Epizyme, PG212), and separated by electrophoresis. The proteins were then transferred onto a PVDF membrane (BIO-RED, 1620177) using a transfer apparatus. After the transfer, the membrane was blocked with 5% non-fat dry milk in TBST buffer (20 mM Tris-HCl, pH 7.5, 150 mM NaCl, and 0.05% Tween-20) for 1 h at room temperature. The membranes were cut horizontally according to the molecular weight (MW) for indicated primary antibodies, and incubated with primary antibody overnight at 4 °C with gentle shaking. The next day, the membrane was washed with TBST buffer and incubated with a secondary antibody conjugated to horseradish peroxidase (HRP) for 1 h at room temperature. After washing, the protein bands were visualized using an enhanced chemiluminescence (ECL) substrate (4 A BIOTECH, 4AW011-200) and imaged using a ChemiDoc XRS + imaging system (Bio-Rad, USA). After visualization, the membrane blots were stripped to remove old primary and secondary antibody using Stripping buffer (Beyotime, P0025B). Then, the membrane can be reprobed with other primary antibodies when the membrane was used to detect the same signal pathway. The primary antibodies were purchased from ABclonal Technology Co.,Ltd. Included: RAGE (A23422), β-actin (AC006), p-Erk (AP0472), Erk (A4782), p-IKKα/β (AP0546), IKKα/β (A2062), IκBα (A11397), p-p65 (AP0123), p65 (A19653), Caspase-9 (A2636). Caspase-3 (A2156), Bcl-2 (A0208), Bax (A0207), cytochrome-c (A0225), E-cadherin (A11509), N-cadherin (A0433), MMP9 (A0289), vimentin (A19607), snail (A5243), HMGB1 (A19529). The secondary antibody included anti-Rabbit, anti-mouse secondary antibody (ABclonal, AS014, AS003). The same gels that were run for separate proteins used the same loading control.

2.7. Cell migration and invasion

Cell migration and invasion were assessed using the Transwell assay (Corning Inc., 14721083). For migration assays, TNBC cells were seeded in the upper chamber of the Transwell insert at a density of 2×10^5 cells per well in serum-free medium with gradient concentrations of peptides, while the lower chamber was filled with medium containing 20% FBS as a chemoattractant. For invasion assays, the Transwell insert was coated with Matrigel (Corning Inc., 354248) prior to cell seeding to mimic the cellular matrix. The following steps were the same as the cell migration assay. Cells were treated with the RP7 for 24 h, and then the inserts were fixed with 4% paraformaldehyde (Servicebio, G1101) for 15 min at room temperature and stained with 0.5% crystal violet (Sigma-Aldrich, C0775) for 10 min. Images were captured by optical inverted microscope (Nikon, Japan), The number of migrated or invaded cells was quantified using ImageJ software (National Institutes of Health, Bethesda, MD, USA).

2.8. Animal model

Six-week-old female nude BALB/c mice, purchased from Guangdong Medical Laboratory Animal Center, were randomly divided into three groups and subcutaneously injected with TNBC cells (5×10^6 cells in 100 μl PBS/mouse) into the left axilla. The animal study was reviewed and approved by the Administrative Committee on Animal Research of the Shenzhen International Graduate School, Tsinghua University (Ethical Development No. 16). The mice were treated with RP7 peptides daily by tail intravenous injection. Bodyweight and tumor sizes were measured and recorded every 2 days. The primary tumor volume was calculated using the formula: (length) × $(\text{width})^2 \times 0.5$. After 22 days of treatment, the mice were sacrificed to collect tumors, blood, and other viscera for further research.

2.9. IHC and HE staining

At the end of animal study, all mice were sacrificed and the tumors were surgically excised. Tumor tissues were fixed in 10% buffered formalin and paraffin-embedded. IHC was conducted according to manufacturer's protocol. Tumor sections were stained with monoclonal antibodies against: Ki67. HMGB1, MMP9 and Caspase 3 (ABclonal Technology Co.,Ltd., A20018, A19529, A0289, A2156). Subsequent operations were performed in accordance with standard immunohistochemical protocols utilizing predetermined optimal primary antibody concentrations, SAB detection, and 3'3'-di-aminobenzidine tetrahydrochloride (DAB, Solarbio, DA1010). Hematoxylin and eosin (H&E) staining was performed on paraffin-embedded tumor tissues with a slice thickness of 6 μm for histological study as previous described.

2.10. TUNEL staining

Apoptosis of the tumor tissues was determined by TUNEL staining, by a commercially available kit (Ribobio, C11012-2). Tumor sections were deparaffinized and dehydrated according to standard protocols. TUNEL reaction mixture containing TdT enzyme and fluorescein-labeled dUTP was added to the sections, and the sections were incubated in a humidified chamber at 37 °C for 1 h in the dark. Nuclei were counterstained with DAPI (1:1000 dilution) (Sigma-Aldrich, D9542) for 10 min. The slides were mounted and analyzed by microscope after staining (Nikon, USA).

2.11. Toxicology assays

When sacrificing the mice, orbital blood samples were collected into 1.5 mL microcentrifuge tubes and stored at 4 °C overnight. The samples were then centrifuged at 10,000 g for 10 min at 4 °C, and the supernatant was collected without the cell pellet. The serum samples were then subjected to a second round of centrifugation to remove any residual cellular debris, and stored at −20 °C until further analysis. The serum was analyzed by the alanine aminotransferase (ALT), aspartate aminotransferase (AST), alkaline phosphatase (ALP) and triglyceride (TG) kits (Jinmei Biotech, China).

2.12. Ethical regulations

All animal studies were approved by the Administrative Committee on Animal Research of Shenzhen International Graduate School, Tsinghua University (Ethical Development no. 16). The patients' biopsy samples were obtained and approved by the Ethics Committees of

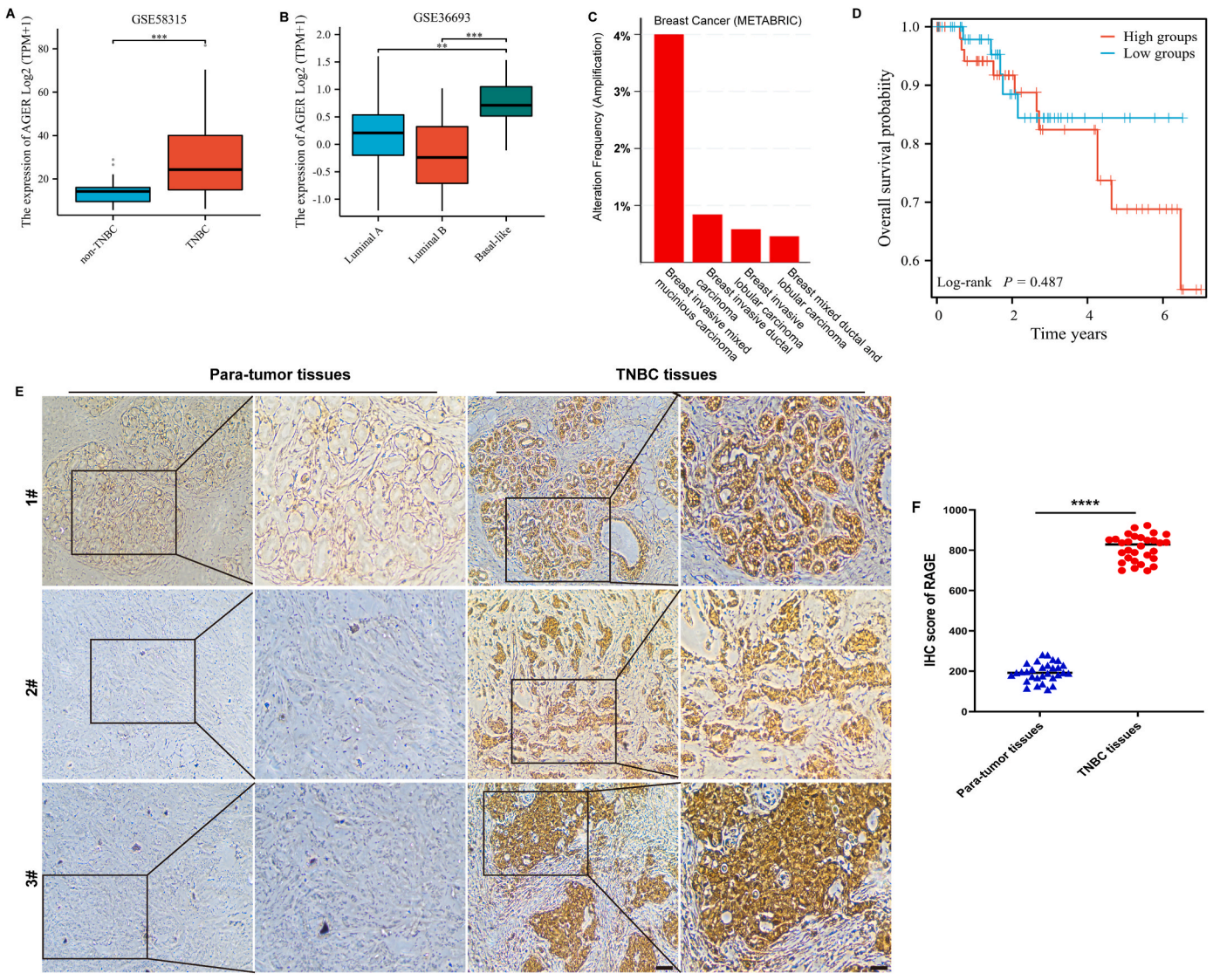

Fig. 1. RAGE is highly expressed in TNBC and is associated with poor progression A, The expression level of RAGE in TNBC and non-TNBC from the GEO database. B, The expression level of RAGE in Basal like, Luminal and Luminal B types breast cancer. *P < 0.05. Significant difference was determined by the student's t-test. C, The gene amplification alteration frequency of RAGE in breast cancer (METABRIC, Nature (2012) & Nat Commun 2016. D, Patients with high RAGE expression have poorer OS compared with patients with low RAGE expression. E, Representative immunohistochemical staining of RAGE in TNBC clinical tissues and para-tumor tissues. Scale bar at left: 100 μm. Scale bar at right: 50 μm. F, Semi-quantitative IHC score of RAGE expression in TNBC clinical tissues and para-tumor tissues. ****p < 0.0001 compared with para-tumor tissues.

Peking University Shenzhen Hospital (Ethical Development no. 28), and written informed consent was obtained from all subjects in this study.

2.13. Statistical analysis

All experiments were repeated a minimum of three times, and the data are presented as mean ± SD. All data was analyzed using Prism 8.0 (GraphPad, Inc.) software. Statistical differences between data groups were evaluated for statistical significance using the *t*-test (comparing two experimental groups) for unpaired data or one-way ANOVA (more than two groups involved). P values less than 0.05 were considered statistically significant.

3. Results

3.1. RAGE is highly expressed in TNBC and is associated with poor progression

To investigate the expression level of RAGE in TNBC, we analyzed several databases. As shown in Fig. 1A, RAGE was found to be significantly highly expressed in TNBC compared to non-TNBC based on the GEO database GSE58135 data. Additionally, analysis of GEO database GSE36693 data showed that RAGE was highly expressed in Basal-like breast (majorly TNBC) cancer when compared with Luminal A and Luminal B subtypes (Fig. 1. B). The METABRIC is a public database including gene expression, gene copy number, gene mutation and clinic data, and aims to classify breast cancer into ten different subtype, which is useful for breast cancer precision therapy. The results in Fig. 1. C showed that the amplification frequency of RAGE was increased in invasive breast cancer (Breast invasive mixed mucinious carcinoma, Breast invasive ductal carcinoma and Breast invasive lobular carcinoma)

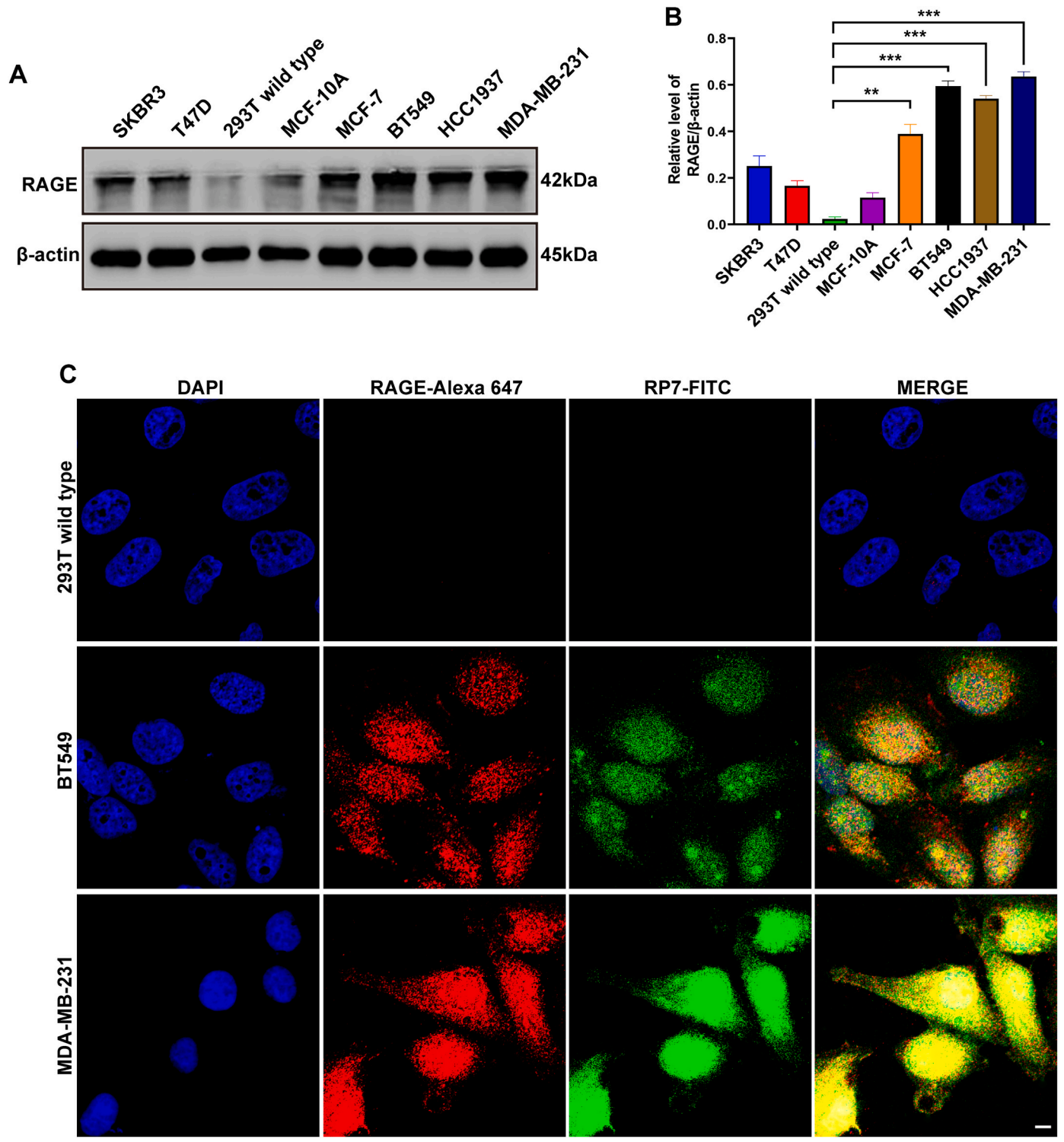

Fig. 2. Identification of the binding ability of RP7 to TNBC. A, The protein expression level of RAGE in 293 T, MCF-10 A, MCF-7 (ER^+), SKBR3 ($HER2^+$), T47D, and TNBC cell lines BT549, MDA-MB-231. B, statistical analysis of western blot in A. C, Confocal image for the co-localization of RP7 and RAGE. Scale bar: 25 μm. The results are representative of three independent experiments and are expressed as the mean ± SD. **$p < 0.01$, ***$p < 0.001$ compared with the 293 T wild type. Significant difference was determined by one-way ANOVA.

when compared with non-invasive breast cancer (Breast mixed ductal and lobular carcinoma). Notably, when compared to the group with low RAGE expression, the worse overall survival (OS) was found in RAGE high expression group (Fig. 1. D). To further identify the expression level of RAGE in TNBC clinic tissue, the IHC staining was performed. The results showed that RAGE was highly expressed in TNBC tissues, while being expressed at a lower level in para-tumor tissues (Fig. 1 E,F). The available data suggests that upregulation of RAGE has clinical significance and is associated with poor prognosis in TNBC. It is likely that RAGE plays a role in TNBC progression.

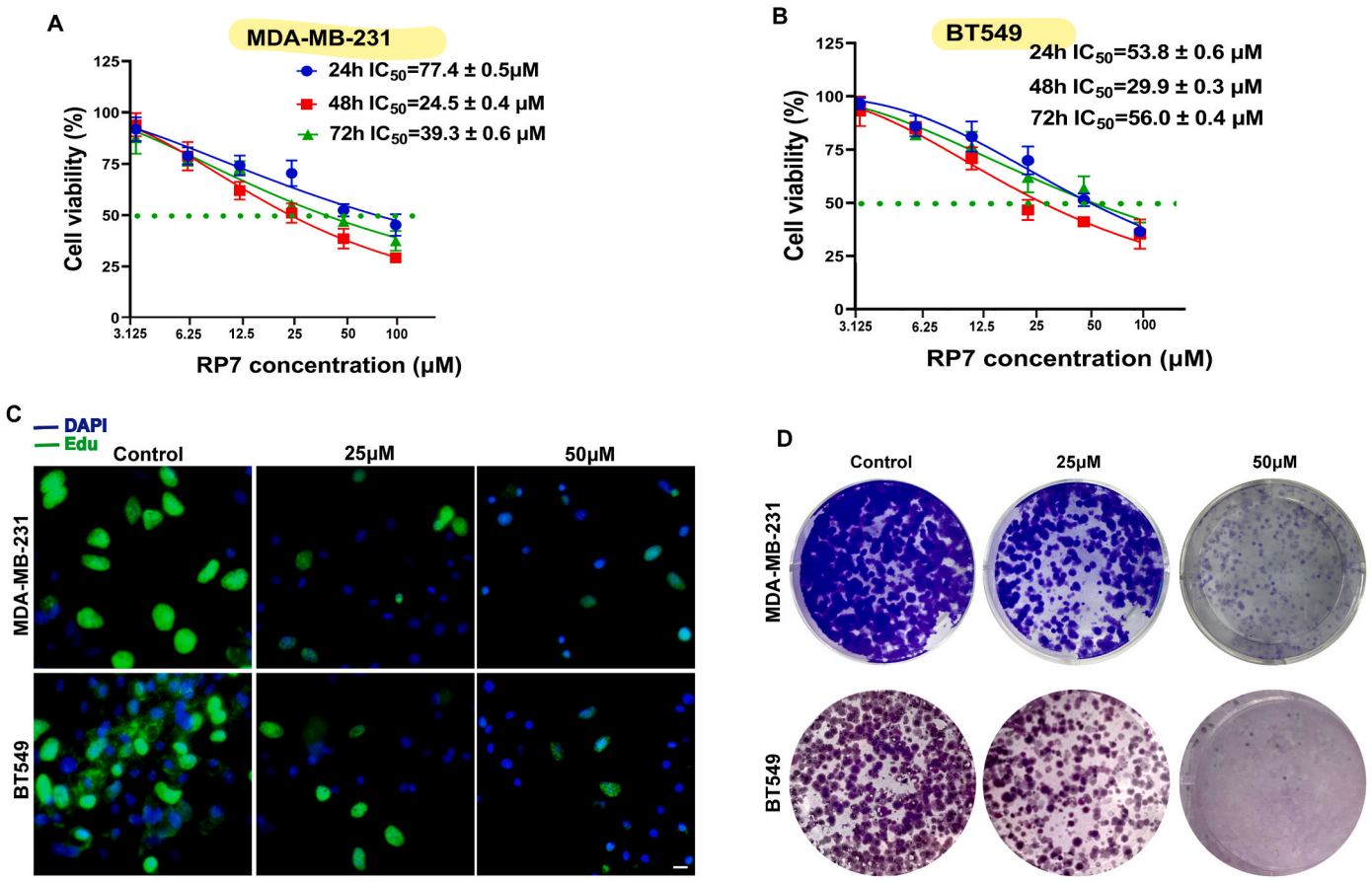

Fig. 3. RP7 suppresses the proliferation of TNBC cells A, The viability of MDA-MB-231 after different RP7 concentrations treatment at 24 h, 48 h, and 72 h. B, The viability of BT549 after different RP7 concentrations treatment at 24 h, 48 h, and 72 h. C, EDU analysis for DNA synthesis in different RP7 concentrations. Scale bar: 100 μm. D, Clone formation assay of MDA-MB-231 and BT549 after RP7 treatment. The results are representative of three independent experiments and are expressed as the mean ± SD.

3.2. Identification the binding ability of RP7 to RAGE

The expression level of RAGE was detected in different cell lines using Western blotting, the results showed that RAGE was overexpressed in breast cancer cell lines compared to 293 T cells and normal breast epithelial cells MCF-10 A. In addition, the expression level of RAGE was found to be significantly higher in TNBC cell lines, such as BT549, HCC 1937, and MDA-MB-231, compared to ER + breast cancer cells MCF-7 and HER2+ breast cancer cells SKBR3, as demonstrated by Western blot analysis (Fig. 2. A, B). Therefore, the RAGE overexpressed cells BT549 and MDA-MB-231 were used for further study. An MTT assay was performed to investigate the anti-proliferation effects of eight RAGE peptides (RP1-8) in MDA-MB-231 cells. Results showed that among the eight peptides, RP7 exhibited the most potent cytotoxic activity when compared to the other seven peptides. (Fig. S1). Thus, the subsequent experiments aimed to investigate the antitumor effects and underlying mechanisms of RP7 in TNBC. HPLC and MS were conducted to purify and authenticate RP7 as shown in Figs. S2A and B. To evaluate the binding ability of RP7 to RAGE, an immunofluorescence assay was performed using 293 T, BT549 and MDA-MB-231 cells. The FITC-labeled RP7 (green) was predominantly observed and could co-locate with RAGE (red) to produce yellow puncta on the membrane of BT549 and MDA-MB-231 cells when compared with RAGE-low expression 293 T cells (Fig. 2. C). These findings suggest that RP7 has the ability to specifically bind to RAGE.

3.3. RP7 suppresses the proliferation of TNBC cells

To evaluate the anticancer activity of RP7, MTT assays were performed on MDA-MB-231 and BT549 cells. As shown in Fig. 3A, the IC50 values of RP7 for MDA-MB-231 at 24, 48, and 72 h were 77.4 μM, 24.5 μM, and 39.3 μM, respectively. For BT549, the IC50 values at 24, 48, and 72 h were 53.8 μM, 29.9 μM, and 56.0 μM, respectively (Fig. 3B). These results suggest that 48 h is the optimal duration for drug treatment and that the RP7 peptide may experience some degradation after 72 h. Additionally, the EDU staining showed that RP7 treatment significantly decreased the DNA synthesis of TNBC cells (Fig. 3C). Furthermore, the colony formation assay indicated that RP7 inhibited the colony formation ability of MDA-MB-231 and BT549 cells compared to the control group (Fig. 3D). These results suggest that RP7 can effectively suppress the proliferation of TNBC cells *in vitro*.

3.4. RP7 inhibits the activation of the Erk1/2/NF-κB pathway

The potential anti-tumor mechanism of RP7 was investigated through immunofluorescence assay and Western blotting. Our findings suggest that RP7 significantly inhibits the nuclear translocation of p65 (Fig. 4A and B). The Western blotting results from MDA-MB-231 (Fig. 4. C) and BT549 (Fig. 4. D) cells demonstrated that RP7 significantly inhibited the phosphorylation of Erk1/2, IKKα/β, IKBα and p65, and inhibited the activity of the Erk1/2/NF-κB pathway. Overall, RP7 can inhibit the entry of p65 into the nucleus, leading to a decrease in the activity of the Erk1/2/NF-κB pathway, which ultimately leads to inhibition of TNBC cell proliferation.

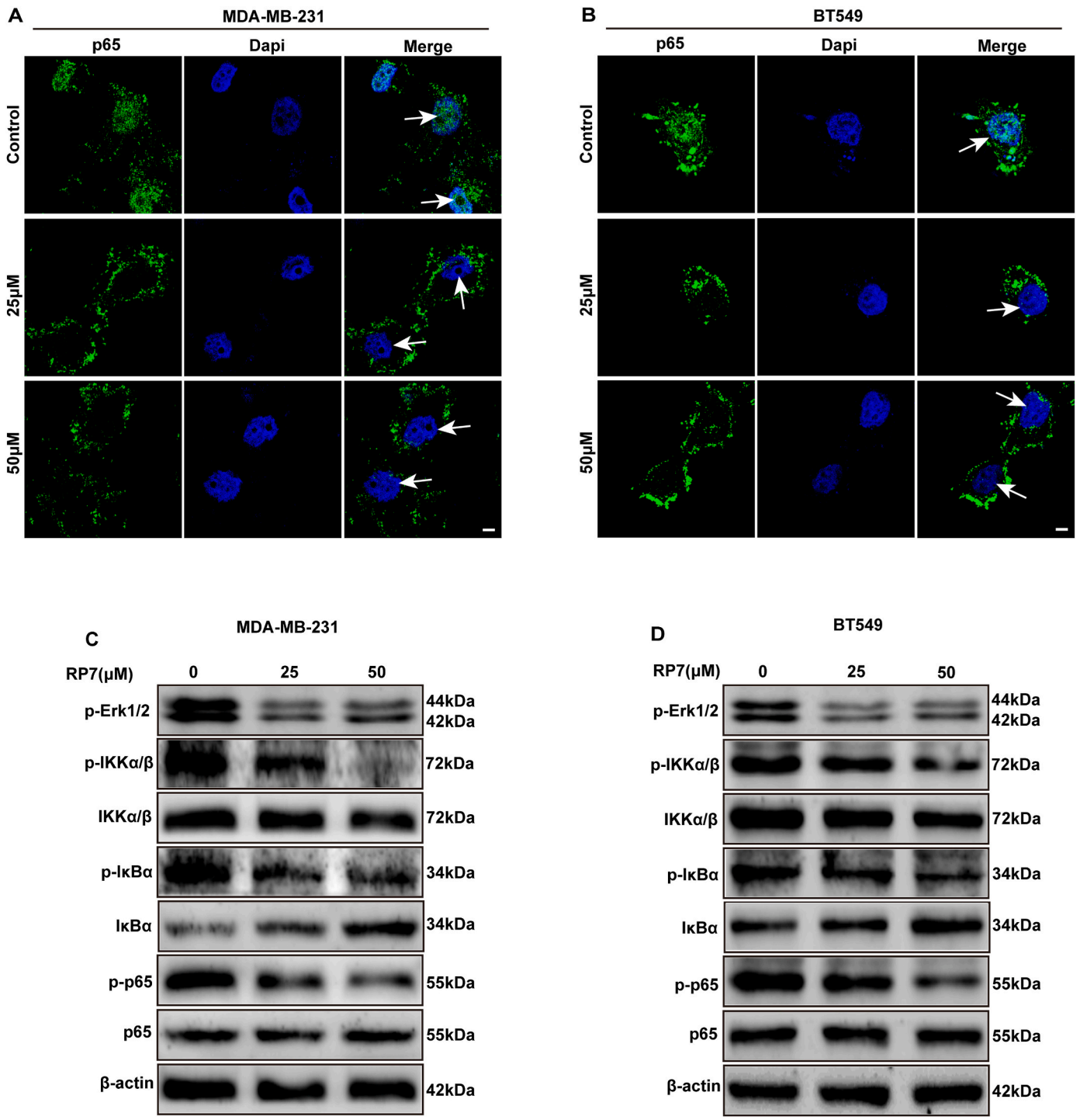

Fig. 4. RP7 inhibits the activity of the Erk1/2/NF-κB pathway. A, Confocal assay of the effect of RP7 on p65 expression in MDA-MB-231. Scale bar: 50 μm. B, Confocal assay of the effect of RP7 on p65 expression in BT549 cells. Scale bar: 50 μm. C, Western blot of the effect of RP7 on Erk1/2/NF-κB pathway in MDA-MB-231. D, Western blot of the effect of RP7 on Erk1/2/NF-κB pathway in BT549. Results are representative of three independent experiments.

3.5. RP7 promotes apoptosis in TNBC cells by decreasing Bcl-2 protein

To further investigate the pro-apoptotic effects of RP7 on TNBC cells, flow cytometry assays were performed. As illustrated in Fig. 5. A-C, RP7 treatment significantly increased the proportion of apoptotic cells in MDA-MB-231 and BT549 cell lines. Furthermore, the immunofluorescence assay demonstrated that RP7 treatment resulted in a significant reduction in Bcl-2 expression in both MDA-MB-231 and BT549 cells (Fig. 5. D and E). The protein levels of cleaved caspase-9, cleaved caspase-3, Bax were all significantly up-regulated, while Bcl-2 was down-regulated by RP7 (Fig. 5. F and G). Moreover, Western blotting analysis revealed that RP7 treatment resulted in a significant decrease in the level of cytochrome C in mitochondria and an increase in the level of cytochrome C in the cytoplasm of TNBC cells. Taken together, these results suggested that RP7 inhibited the Bcl-2 and increased the Bax, which facilitated the release of cytochrome C from mitochondria into the cytoplasm, ultimately activating caspase-9/caspase-3 mediated apoptosis in TNBC cells.

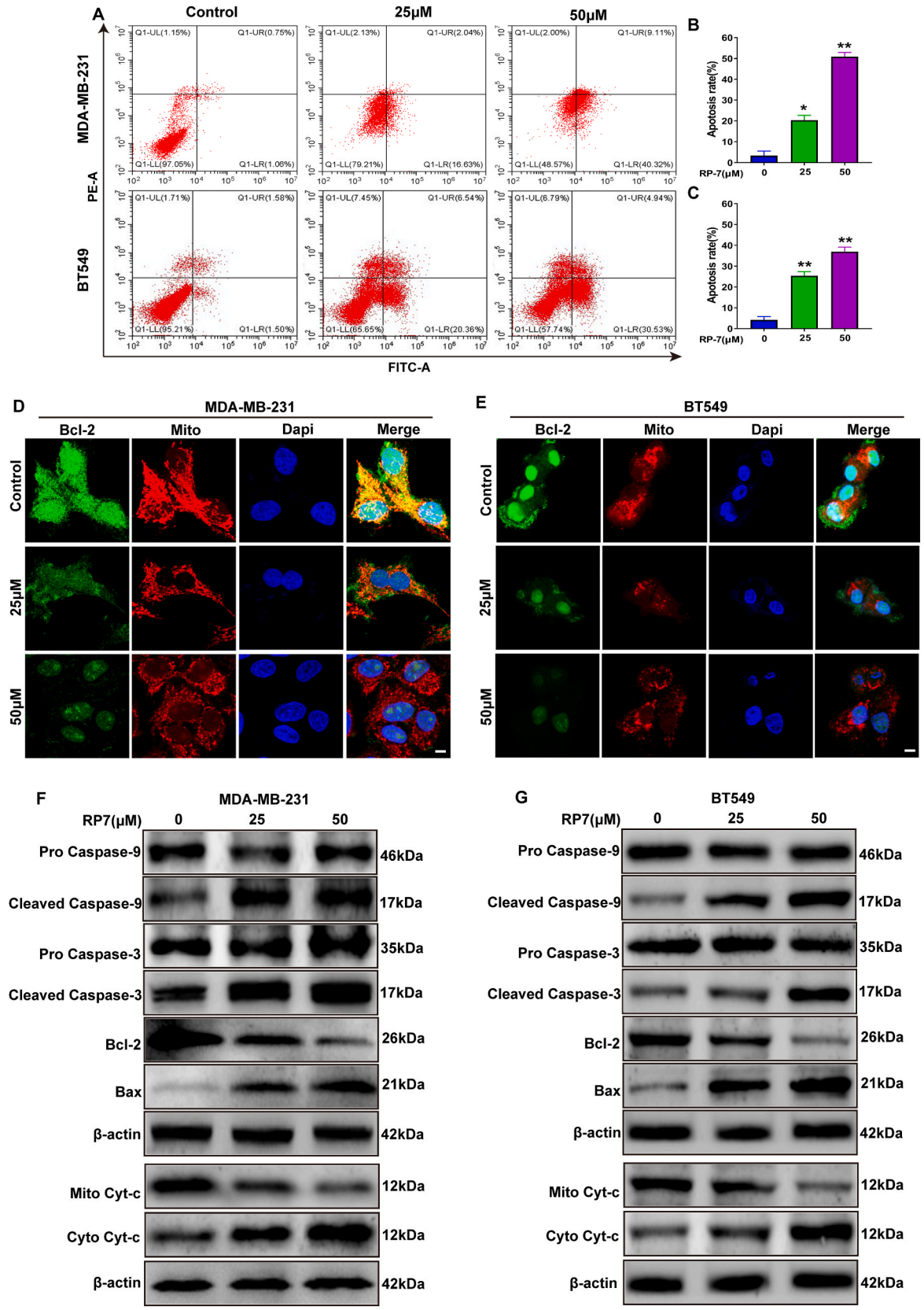

Fig. 5. RP7 promotes apoptosis in TNBC cells by inhibiting Bcl-2 expression. A, Flow cytometry assay of MDA-MB-231 and BT549 cells apoptosis after RP7 treatment; B, Statistical results of apoptosis in MDA-MB-231. C, Statistical results of apoptosis in BT549. D, Confocal assay of the effect of RP7 on Bcl-2 expression in MDA-MB-231. Scale bar: 50 μm. E, Confocal assay of the effect of RP7 on Bcl-2 expression in BT549 cells. Scale bar: 50 μm. F, Western blot of RP7 on the Caspase-9/caspase-3 pathway in MDA-MB-23. G, Western blot of RP7 on the Caspase-9/caspase-3 pathway in BT549 cells. Results are representative of three independent experiments and are expressed as the mean ± SD. *P < 0.05; **P < 0.01, compared to 0 μM. Significant difference was determined by one-way ANOVA.

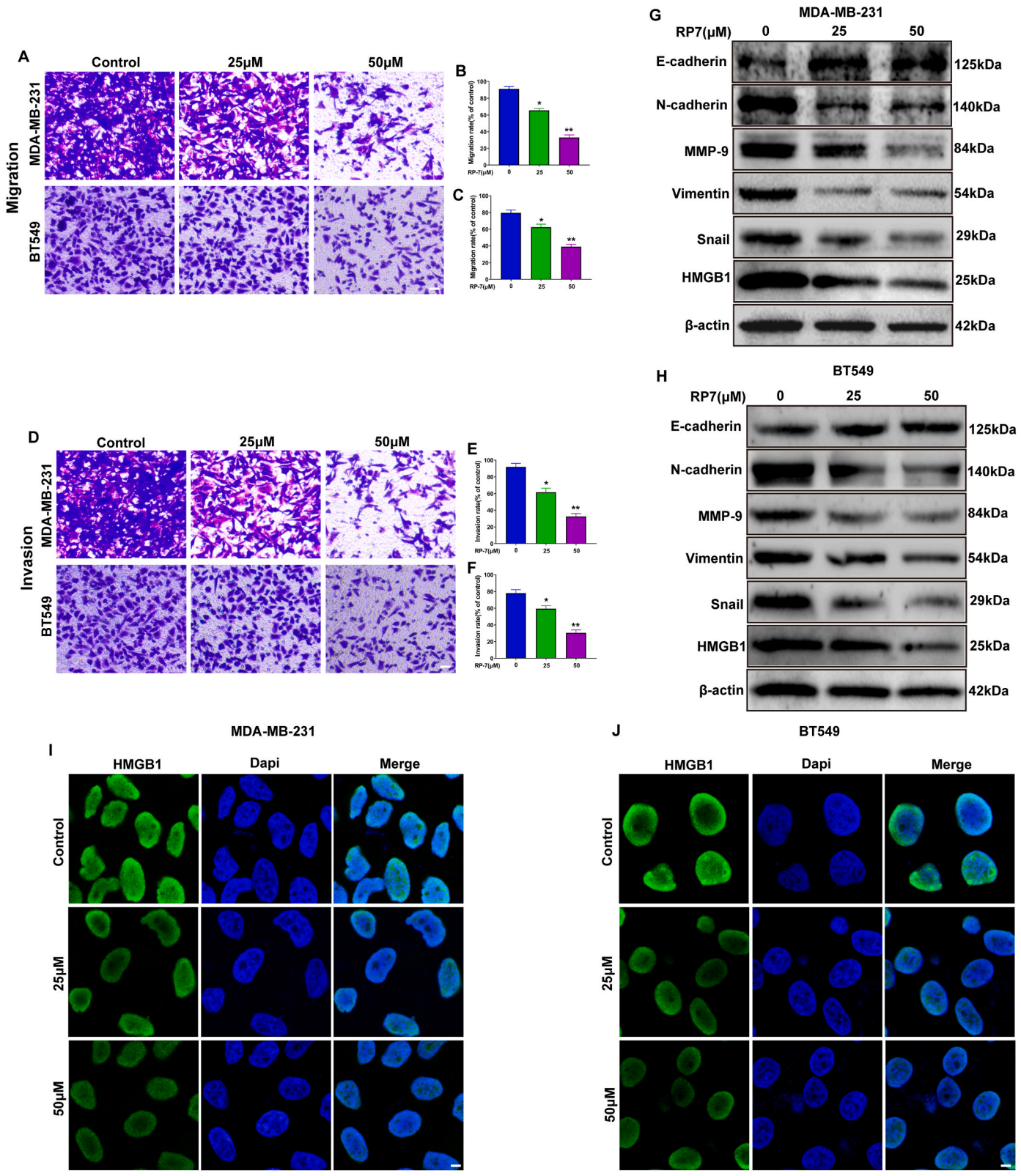

Fig. 6. RP7 inhibits TNBC cell invasion and migration by blocking the HMGB1/EMT signaling pathway. A, The effect of RP7 on the migration ability of MDA-MB-231 and BT549. Scale bar: 125 μm. B, Statistics of the migration ability of MDA-MB-231 cells after RP7 treatment; C, Statistics of the migration ability of BT549 cells after RP7 treatment. D, The effect of RP7 on the invasion ability of TNBC cells. Scale bar: 125 μm. E, Statistics of the invasion ability of MDA-MB-231 cells after RP7 treatment. Scale bar: 125 μm. F, Statistics of the invasion ability of BT549 cells after RP7 treatment. Scale bar: 125 μm. G, The effect of RP7 on HMGB1/EMT signaling pathway-related proteins in MDA-MB-231 cells. H, The effect of RP7 on HMGB1/EMT signaling pathway-related proteins in BT549. I, Confocal assay of the effect of RP7 on HMGB1 expression in MDA-MB-231. Scale bar: 50 μm. J, Confocal assay of the effect of RP7 on HMGB1 expression in BT549 cells. Scale bar: 50 μm. Results are representative of three independent experiments and are expressed as the mean ± SD. *$P < 0.05$; **$P < 0.01$, compared to 0 μM. Significant difference was determined by one-way ANOVA.

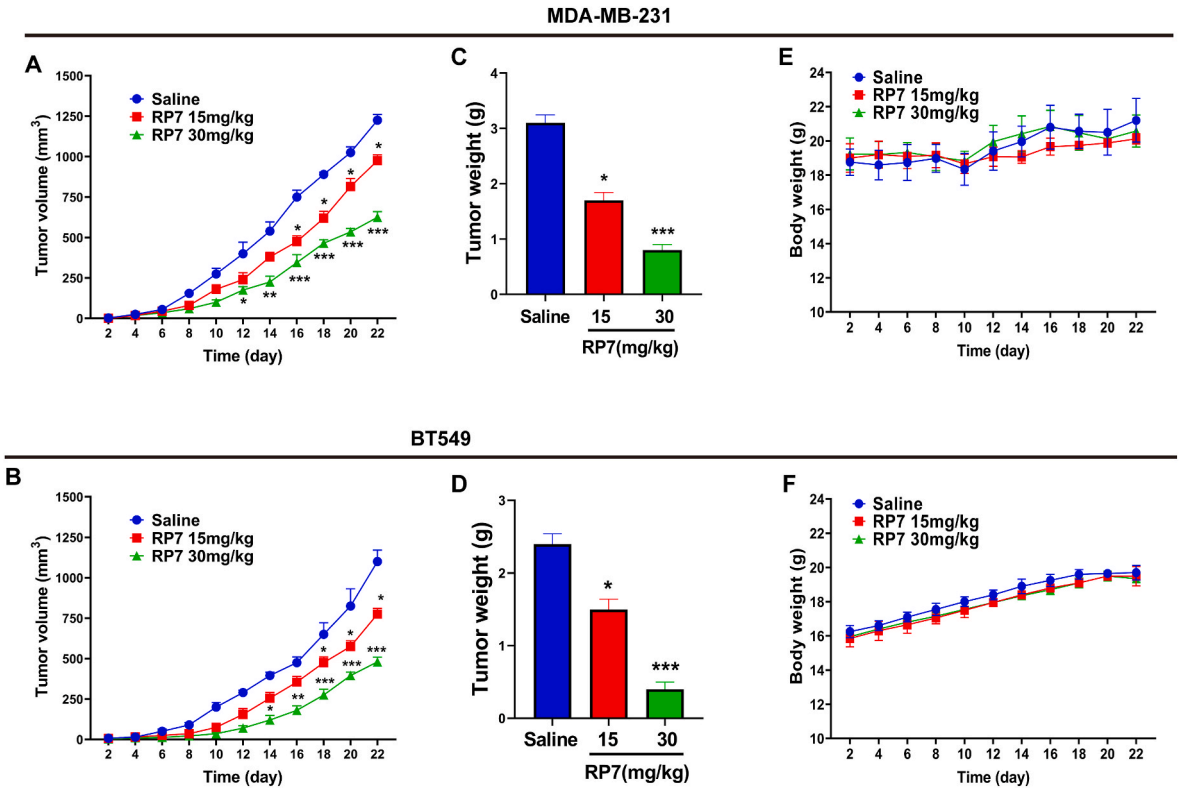

Fig. 7. RP7 significantly inhibited the formation of TNBC. A, The tumor volume growth curve of MDA-MB-231 xenograft tumor models. B, The tumor volume growth curve of BT549 xenograft tumor models. C, The tumor weight of MDA-MB-231 xenograft tumor models. D, The tumor weight of BT549 xenograft tumor models. E, Body weight of MDA-MB-231 xenograft tumor models in different dosing groups. F, Body weight of BT549 xenograft tumor models in different dosing groups. Results are representative of three independent experiments and are expressed as the mean ± SD. *p < 0.05, **p < 0.01, ***p < 0.001 compared with the saline group. Significant difference was determined by one-way ANOVA.

3.6. RP7 inhibits TNBC cells invasion and migration by blocking the HMGB1/EMT signaling pathway

To investigate the potential inhibitory effect of RP7 on the invasion and migration of TNBC cells, transwell assays were performed. As shown in Fig. 6. A-F, RP7 treatment resulted in a significant inhibition of TNBC cell migration and invasion in a dose-dependent manner. In addition, the Western blotting results revealed that the protein expression levels of HMGB1, N-cadherin, vimentin, and snail were all decreased, while E-cadherin was increased after RP7 treatment (Fig. 6G and H). Confocal images further confirmed that RP7 treatment led to a decrease in the expression level of HMGB1 in both MDA-MB-231 and BT549 cells. Generally, these results indicated that RP7 inhibitd TNBC cells migration and invasion through blocking HMGB1/EMT signaling pathway.

3.7. RP7 significantly inhibits the growth of TNBC in xenograft model

In the in-vivo study, MDA-MB-231 and BT549 cell lines were implanted into Balb/c nude mice to establish the TNBC xenograft model. RP7 treatment resulted in a significant reduction in tumor volume and weight when compared with the control group (Fig. 7 A-D). The body weight of mice in the different dosing groups did not show any significant difference when compared to the control group (Fig. 7 E-F). As shown in Fig. S3. A-D, no significant difference was observed in the ELISA results of ALT, AST, ALP and TG after RP7 administration. Moreover, the HE staining for heart, liver, spleen, lung, and kidney tissues after RP7 administration indicated no obvious toxicity of RP7 to mice (Fig. S3. E and F). These results suggested that RP7 could significantly inhibit the growth of TNBC with no obvious toxicity.

3.8. RP7 promotes the apoptosis of TNBC in vivo

In Fig. 8. A and B, Consistent with the *in vitro* results, the *in vivo* study showed that the RP7-treated group exhibited decreased expression levels of Ki67, HMGB1, and MMP-9, while caspase-3 expression was increased compared to the control group. Moreover, more apoptotic tumor cells were detected in RP7-treated group (Fig. 8. C and D). These results indicated that RP7 could inhibit TNBC growth and metastasis, while promoted TNBC apoptosis *in vivo*.

4. Discussion

Traditionally, chemotherapy has long been the unique available therapeutic option for TNBC, given its aggressive behavior and poor prognosis compared to other subtypes of breast cancer (Bianchini et al., 2022; Li et al., 2023). Personalized treatment strategies targeting molecular tumor-specific alterations would be the most effective approach to treat TNBC, due to its heterogeneity and the fact that 60–70% of patients do not fully respond to chemotherapy (Bianchini et al., 2016; Won and Spruck, 2020; Li et al., 2021). While TNBC is traditionally defined as breast cancer that lacks expression of estrogen receptor (ER), progesterone receptor (PR), and HER2, recent advances in omics technologies have highlighted the clinical and molecular heterogeneity of this disease, leading to the development of novel targeted agents (Neophytou et al., 2018). In this study, we demonstrated that high expression of RAGE is closely associated with clinical progression of TNBC. Furthermore, we found that the novel RAGE antagonist peptide RP7 has the ability to inhibit TNBC cell proliferation, migration, and invasion both *in vitro* and *in vivo*. Our study has indicated that RAGE is a potential target for TNBC, and that the RAGE antagonist peptide RP7 shows promise as an effective anticancer drug for TNBC.

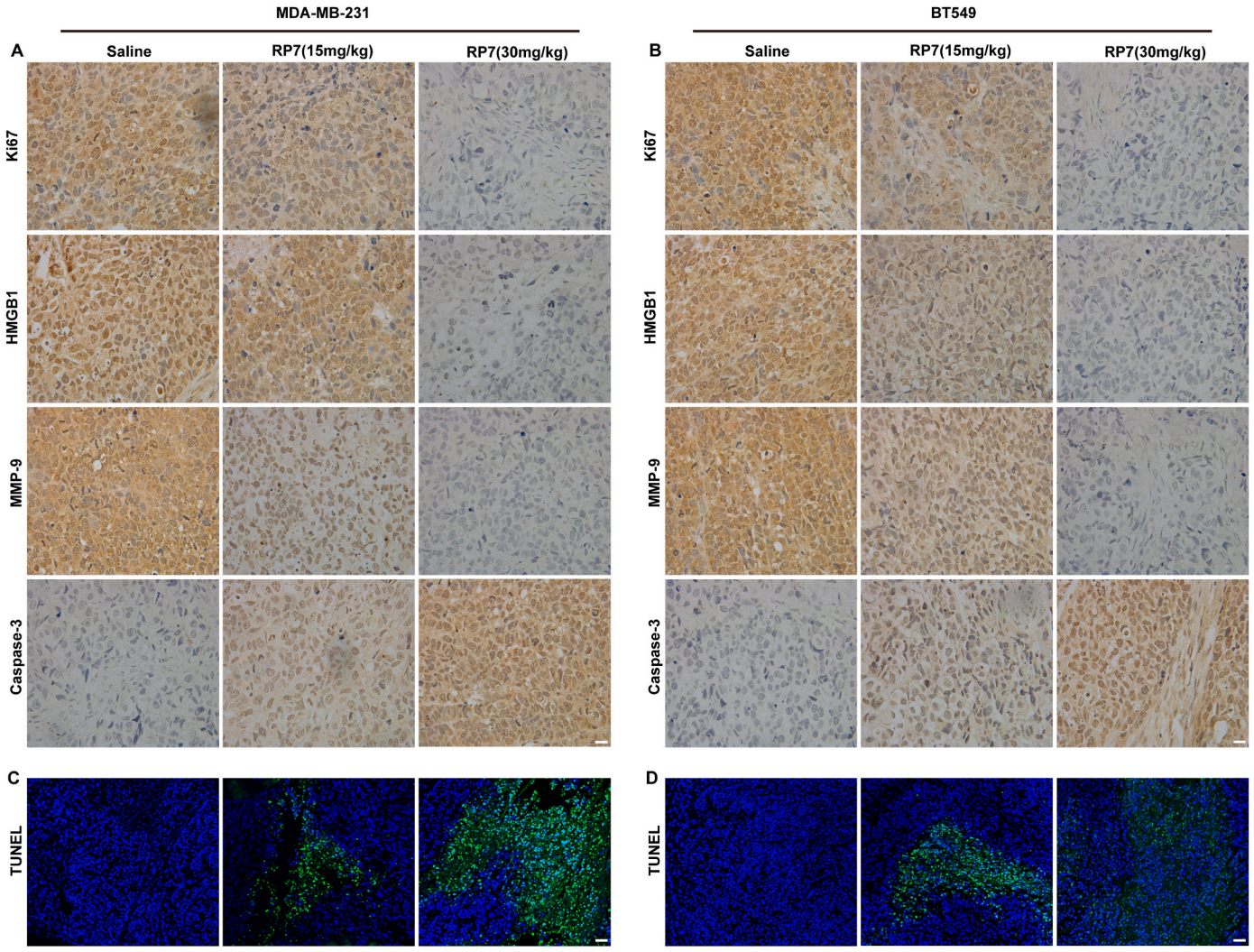

Fig. 8. RP7 promotes apoptosis in TNBC *in vivo*. A, IHC assay of Ki67, HMGB1, MMP-9, and Caspase-3 in MDA-MB-231 xenograft tumor models. Scale bar: 100 μm. B, IHC assay of Ki67, HMGB1, MMP-9, and Caspase-3 in BT549 xenograft tumor models. Scale bar: 100 μm. C, TUNEL assay of MDA-MB-231 xenograft tumor models. Scale bar: 125 μm. D, TUNEL assay of BT549 xenograft tumor models. Scale bar: 125 μm. Results are representative of three independent experiments.

In a number of contexts, the activation of the NF-κB pathway can promote cell apoptosis, it is generally recognized as a pro-survival factor that plays a critical role in response to cellular stress (Khandelwal et al., 2011). Bottero et al. firstly found that IκBα and the NF-κB p65 subunit allocated in mitochondria in Jurkat cells (Bottero et al., 2001). Following study uncovered the role of NF-κB pathway in apoptosis. Upon activation of the NF-κB pathway, IκB is degraded, leading to the translocation of the remaining NF-κB dimer, which may include the p65/p50 or p50/p50 subunit, into the nucleus and mitochondria. Once it enters the mitochondria, the activated NF-κB induces the release of cytochrome *c*, ultimately triggering the caspase cascade and programmed cell death (Albensi, 2019). Herein, RP7 can inhibit the activation of the NF-κB pathway by blocking the phosphorylation of IKKα/β, IKBα, and p65. This is achieved through the inhibition of ERK1/2 activation.

Apoptosis is an ordered and orchestrated cell death that occurs in normal physiological or pathological conditions (Obeng, 2021). Apoptosis is tightly induced by two core pathways, the extrinsic and intrinsic pathways, both of which ultimately lead to the same outcome (D'Arcy, 2019). The release of cytochrome *c* from the mitochondria into the cytoplasm is a crucial step in activating the intrinsic apoptosis pathway, ultimately leading to the formation of the apoptosome and activation of caspase 3 (Carneiro and El-Deiry, 2020). In the extrinsic pathway, caspase 9 initiates the final stage of apoptosis which is then executed by caspase 3, followed by the activation of cytoplasmic endonuclease, ultimately leading to cell death (Ebert et al., 2020). Here, our findings indicate that inhibition of RAGE by RP7 can suppress the activation of the NF-κB pathway, eventually inducing apoptosis in TNBC cells. Specifically, RP7 treatment led to a decline in Bcl 2 expression within mitochondria, while increasing Bax expression in TNBC cells. In downstream, RP7 activated the intrinsic apoptosis pathway, promoting the release of cytochrome C and the activation of caspase 9/3, and ultimately inducing apoptosis. Consistent with results *in vivo*, the results of the immunohistochemistry analysis demonstrated an increase in caspase-3 expression in the tumor tissue of the mice. Thus, our study was the first to confirm that RP7 could inhibit RAGE and suppress TNBC cell proliferation by inducing apoptosis.

RAGE is reported to be closely associated with various cancers including liver, pancreatic, colorectal, gastric and lung cancer (Abe and Yamagishi, 2008; Allmen et al., 2008). Particularly, hypoxia-induced upregulation of RAGE enhances invasion and migration of tumor cells via the phosphorylation of Erk1/2 and nuclear translocation of NF-kB (Tafani et al., 2011). Certain researches have demonstrated the potential function of RAGE in breast cancer *in vitro* (Ghavami et al., 2008; Sharaf et al., 2015). Moreover, a recent study has provided evidence for the therapeutic potential of RAGE antagonists in breast cancer based on

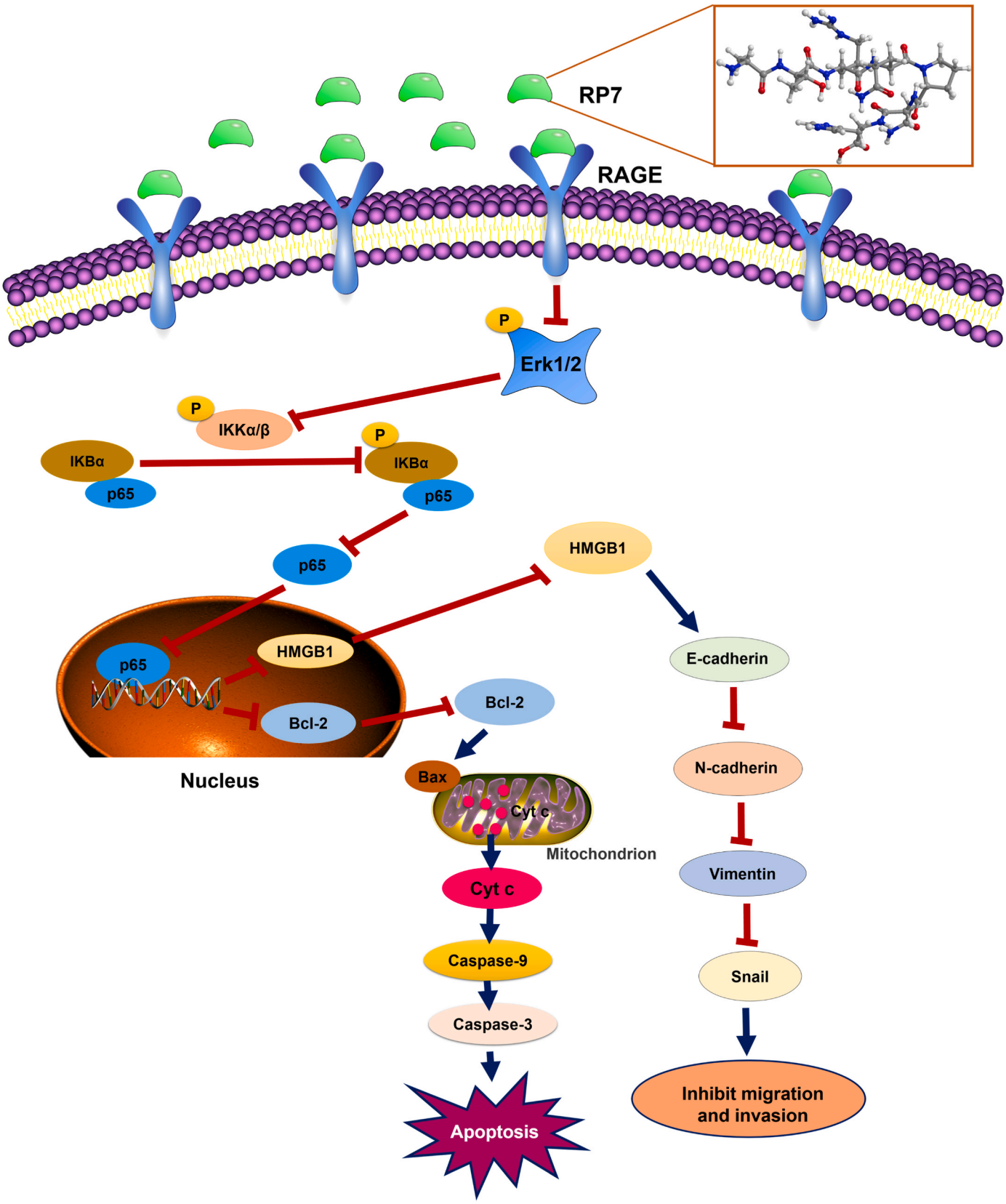

Fig. 9. Schema showing a proposed mechanism of RP7. As the RAGE antagonist peptide, RP7 blocks the phosphorylation of ERK1/2, and further reduces the phosphorylation of IKKα/β, IKBα and p65, result in preventing the entry of p65 into the nucleus. The reduction of p65 in the nucleus decreases the transcriptional expression of Bcl-2. The reduced Bcl-2 then increases the activity of Bax, which promotes the release of cytochrome C from the mitochondria into the cytoplasm, where the cytoplasm cytochrome C further activated caspase-9/caspase-3 pathway to induce TNBC cells apoptosis. Meanwhile, RP7 can decrease the protein level of HMGB1 and blocks the EMT signaling pathways to inhibit the migration and invasion of TNBC cells.

preclinical data. The study showed that novel small molecule inhibitors, such as FPS-ZM1, that target RAGE significantly impaired the metastasis of invasive breast cancer both *in vitro* and *in vivo* (Kwak et al., 2017). Recent studies have revealed that the HMGB1 acts as a novel mediator of EMT to accelerate metastasis (Lv et al., 2019; Qu et al., 2019). In present study, RP7 was found to block RAGE and downregulate HMGB1 expression, thereby inhibiting the EMT pathway and suppressing TNBC cell invasion and migration. More importantly, RP7 also displayed a certain therapeutic effect in the TNBC xenograft model, and the volume of the tumor was notably reduced after RP7 treatment with no significant weight loss. This indicates that RP7 is safe to administer *in vivo* and does not have any apparent toxicity.

5. Conclusions

In summary, we explored the association between RAGE and TNBC development by using bioinformatics, and firstly applied the 7-mer peptide RP7 to inhibit TNBC growth both *in vitro* and *in vivo* through activating apoptosis and inhibiting migration and invasion (Fig. 9). In brief, RP7 inhibited the phosphorylation of ERK1/2 and downstream targets including IKKα/β, IKBα and p65, resulting in the inhibition of p65 nuclear translocation. This led to decreased expression of Bcl-2 and HMGB1. The reduction of Bcl-2 by RP7 led to an increase in Bax expression, which facilitated the release of cytochrome C from the mitochondria into the cytoplasm. This, in turn, activated the caspase-9/caspase-3 pathway, ultimately inducing apoptosis in TNBC cells. Meanwhile, the reduced HMGB1 in RP7-treated cells inhibited the EMT signaling pathway and blocked the migration and invasion of TNBC cells. Collectively, our study indicated that RAGE was a potential target for TNBC, and RP7 was a promising therapeutic agent for TNBC clinical treatment.

CRediT authorship contribution statement

Xiaoyong Dai: designed the study, performed the experiments, analyzed the data, and revised the manuscript. **Yibo Hou:** performed the experiments and wrote the manuscript. **Ting Deng:** performed the experiments and wrote the manuscript. **Gaoyang Lin:** assisted the animal experiments and analyzed, the data. **Yuanxiong Cao:** revised the manuscript, and, analyzed the data. **Guiyuan Yu:** performed the experiments. **Wei Wei:** provided clinical samples and revised the manuscript. **Qing Zheng:** revised the manuscript. **Laiqiang Huang:** designed the study, analyzed the data, and revised the manuscript. **Shaohua Ma:** designed the study, analyzed the data, and revised the manuscript. All authors read and approved the final manuscript.

Declaration of competing interest

The authors declare that they have no known competing financial interests or personal relationships that could have appeared to influence the work reported in this paper.

Data availability

Data will be made available on request.

Acknowledgements

This work was supported by funding from the National Natural Science Foundation of China (82341019), Shenzhen Science and Technology Innovation Commission Key Projects of Fundamental Research and Program for Building Shenzhen City, State Key Laboratories (JCYJ20180508153013853, WDZC20200821141349001). We thank the appropriate specimen donors and research groups for their contributions.

Appendix A. Supplementary data

Supplementary data to this article can be found online at https://doi.org/10.1016/j.ejphar.2023.175861.

References

Abe, R., Yamagishi, S., 2008. AGE-RAGE system and carcinogenesis. Curr. Pharmaceut. Des. 14, 940–945. https://doi.org/10.2174/138161208784139765.
Ahmad, S., Khan, H., Siddiqui, Z., et al., 2018. AGEs, RAGEs and s-RAGE; friend or foe for cancer. Semin. Cancer Biol. 49, 44–55. https://doi.org/10.1016/j.semcancer.2017.07.001.
Albensi, B.C., 2019. What is nuclear factor kappa B (NF-κB) doing in and to the mitochondrion? Front. Cell Dev. Biol. 7, 154. https://doi.org/10.3389/fcell.2019.00154.
Allmen, E.U., Koch, M., Fritz, G., et al., 2008. V domain of RAGE interacts with AGEs on prostate carcinoma cells. Prostate 68 (7), 748–758. https://doi.org/10.1002/pros.20736.
Azizan, N., Suter, M.A., Liu, Y., et al., 2017. RAGE maintains high levels of NFκB and oncogenic Kras activity in pancreatic cancer. Biochem. Biophys. Res. Commun. 493 (1), 592–597. https://doi.org/10.1016/j.bbrc.2017.08.147.
Bianchini, G., Balko, J.M., Mayer, I.A., et al., 2016. Triple-negative breast cancer: challenges and opportunities of a heterogeneous disease. Nat. Rev. Clin. Oncol. 13 (11), 674–690. https://doi.org/10.1038/nrclinonc.2016.66.
Bianchini, G., De Angelis, C., Licata, L., et al., 2022. Treatment landscape of triple-negative breast cancer - expanded options, evolving needs. Nat. Rev. Clin. Oncol. 19 (2), 91–113. https://doi.org/10.1038/s41571-021-00565-2.
Bottero, V., Busuttil, V., Loubat, A., et al., 2001. Activation of nuclear factor kappaB through the IKK complex by the topoisomerase poisons SN38 and doxorubicin: a brake to apoptosis in HeLa human carcinoma cells. Cancer Res. 61 (21), 7785–7791.
Boyle, P., 2012. Triple-negative breast cancer: epidemiological considerations and recommendations. Ann. Oncol. 23 (Suppl. 6), vi7–12.
Cai, C., Dai, X., Zhu, Y., et al., 2016. A specific RAGE-binding peptide biopanning from phage display random peptide library that ameliorates symptoms in amyloid β peptide-mediated neuronal disorder. Appl. Microbiol. Biotechnol. 100 (2), 825–835. https://doi.org/10.1007/s00253-015-7001-7.
Carneiro, B.A., El-Deiry, W.S., 2020. Targeting apoptosis in cancer therapy. Nat. Rev. Clin. Oncol. 17 (7), 395–417. https://doi.org/10.1038/s41571-020-0341-y.
D'Arcy, M.S., 2019. Cell death: a review of the major forms of apoptosis, necrosis and autophagy. Cell Biol. Int. 43 (6), 582–592. https://doi.org/10.1002/cbin.11137.
Ebert, G., Lopaticki, S., O'Neill, M.T., et al., 2020. Targeting the extrinsic pathway of hepatocyte apoptosis promotes clearance of plasmodium liver infection. Cell Rep. 30 (13), 4343–4354.e4. https://doi.org/10.1016/j.celrep.2020.03.032.
Ghavami, S., Rashedi, I., Dattilo, B.M., et al., 2008. S100A8/A9 at low concentration promotes tumor cell growth via RAGE ligation and MAP kinase-dependent pathway. J. Leukoc. Biol. 83 (6), 1484–1492. https://doi.org/10.1189/jlb.0607397.
Gluz, O., Liedtke, C., Gottschalk, N., et al., 2009. Triple-negative breast cancer–current status and future directions. Ann. Oncol. 20 (12), 1913–1927. https://doi.org/10.1093/annonc/mdp492.
Howard, F.M., Olopade, O.I., 2021. Epidemiology of triple-negative breast cancer: a review. Cancer J. 27 (1), 8–16.
Hudson, B.I., Lippman, M.E., 2018. Targeting RAGE signaling in inflammatory disease. Annu. Rev. Med. 69, 349–364. https://doi.org/10.1146/annurev-med-041316-085215.
Ishiguro, H., Nakaigawa, N., Miyoshi, Y., et al., 2005. Receptor for advanced glycation end products (RAGE) and its ligand, amphoterin are overexpressed and associated with prostate cancer development. Prostate 64 (1), 92–100. https://doi.org/10.1002/pros.20219.
Khandelwal, N., Simpson, J., Taylor, G., et al., 2011. Nucleolar NF-κB/RelA mediates apoptosis by causing cytoplasmic relocalization of nucleophosmin. Cell Death Differ. 18 (12), 1889–1903. https://doi.org/10.1038/cdd.2011.79.
Kuniyasu, H., Oue, N., Wakikawa, A., et al., 2002. Expression of receptors for advanced glycation end-products (RAGE) is closely associated with the invasive and metastatic activity of gastric cancer. J. Pathol. 196 (2), 163–170. https://doi.org/10.1002/path.1031.
Kwak, T., Drews-Elger, K., Ergonul, A., et al., 2017. Targeting of RAGE-ligand signaling impairs breast cancer cell invasion and metastasis. Oncogene 36 (11), 1559–1572. https://doi.org/10.1038/onc.2016.324.
Lai, W., Li, X., Kong, Q., et al., 2021. Extracellular HMGB1 interacts with RAGE and promotes chemoresistance in acute leukemia cells. Cancer Cell Int. 21 (1), 700. https://doi.org/10.1186/s12935-021-02387-9.
Li, Y., Zhan, Z., Yin, X., et al., 2021. Targeted therapeutic strategies for triple-negative breast cancer. Front. Oncol. 11, 731535 https://doi.org/10.3389/fonc.2021.731535/.
Li, J., Xia, Q., Di, C., et al., 2023. Tumor cell-intrinsic CD96 mediates chemoresistance and cancer stemness by regulating mitochondrial fatty acid β-oxidation. Adv. Sci. 10 (7), e2202956.
Lin, N.U., Claus, E., Sohl, J., et al., 2008. Sites of distant recurrence and clinical outcomes in patients with metastatic triple-negative breast cancer: high incidence of central nervous system metastases. Cancer 113 (10), 2638–2645. https://doi.org/10.1002/cncr.23930.
Lv, D.J., Song, X.L., Huang, B., et al., 2019. HMGB1 promotes prostate cancer development and metastasis by interacting with brahma-related gene 1 and

activating the akt signaling pathway. Theranostics 9 (18), 5166–5182. https://doi.org/10.7150/thno.33972.
Moynagh, P.N., 2005. The NF-kappaB pathway. J. Cell Sci. 118 (Pt 20), 4589–4592. https://doi.org/10.1242/jcs.02579.
Neophytou, C., Boutsikos, P., Papageorgis, P., 2018. Molecular mechanisms and emerging therapeutic targets of triple-negative breast cancer metastasis. Front. Oncol. 8, 31. https://doi.org/10.3389/fonc.2018.00031.
Obeng, E., 2021. Apoptosis (programmed cell death) and its signals - a review. Braz. J. Biol. 81 (4), 1133–1143.
Oeckinghaus, A., Ghosh, S., 2009. The NF-kappaB family of transcription factors and its regulation. Cold Spring Harbor Perspect. Biol. 1 (4), a000034.
Palanissami, G., Paul, S.F.D., 2018. RAGE and its ligands: molecular interplay between glycation, inflammation, and hallmarks of cancer-a review. Horm. Cancer 9 (5), 295–325. https://doi.org/10.1007/s12672-018-0342-9.
Qu, J., Zhang, Z., Zhang, P., et al., 2019. Downregulation of HMGB1 is required for the protective role of Nrf 2 in EMT-mediated PF. J. Cell. Physiol. 234 (6), 8862–8872. https://doi.org/10.1002/jcp.27548.
Sharaf, H., Matou-Nasri, S., Wang, Q., et al., 2015. Advanced glycation endproducts increase proliferation, migration and invasion of the breast cancer cell line MDA-MB-231. Biochim. Biophys. Acta 1852 (3), 429–441. https://doi.org/10.1016/j.bbadis.2014.12.009.
Somensi, N., Brum, P.O., de Miranda Ramos, V., et al., 2017. Extracellular HSP70 activates ERK1/2, NF-kB and pro-inflammatory gene transcription through binding with RAGE in A549 human lung cancer cells. Cell. Physiol. Biochem. 42 (6), 2507–2522. https://doi.org/10.1159/000480213.
Sun, S.C., 2011. Non-canonical NF-κB signaling pathway. Cell Res. 21 (1), 71–85. https://doi.org/10.1038/cr.2010.177.
Tafani, M., Schito, L., Pellegrini, L., et al., 2011. Hypoxia-increased RAGE and P2X7R expression regulates tumor cell invasion through phosphorylation of Erk1/2 and Akt and nuclear translocation of NF-{kappa}B. Carcinogenesis 32 (8), 1167–1175. https://doi.org/10.1093/carcin/bgr101.
Vallabhapurapu, S., Karin, M., 2009. Regulation and function of NF-kappaB transcription factors in the immune system. Annu. Rev. Immunol. 27, 693–733. https://doi.org/10.1146/annurev.immunol.021908.132641.
Wang, J., Li, R., Peng, Z., et al., 2020. HMGB1 participates in LPS-induced acute lung injury by activating the AIM2 inflammasome in macrophages and inducing polarization of M1 macrophages via TLR2, TLR4, and RAGE/NF-κB signaling pathways. Int. J. Mol. Med. 45 (1), 61–80. https://doi.org/10.3892/ijmm.2020.4530.
Wautier, J.L., Zoukourian, C., Chappey, O., et al., 1996. Receptor-mediated endothelial cell dysfunction in diabetic vasculopathy. Soluble receptor for advanced glycation end products blocks hyperpermeability in diabetic rats. J. Clin. Invest. 97 (1), 238–243. https://doi.org/10.1172/JCI118397.
Wolff, A.C., Hammond, M.E., Hicks, D.G., et al., 2013. Recommendations for human epidermal growth factor receptor 2 testing in breast cancer: American Society of Clinical Oncology/College of American Pathologists clinical practice guideline update. J. Clin. Oncol. 31 (31), 3997–4013.
Won, K.A., Spruck, C., 2020. Triple-negative breast cancer therapy: current and future perspectives (Review). Int. J. Oncol. 57 (6), 1245–1261.
Yan, S.D., Chen, X., Fu, J., et al., 1996. RAGE and amyloid-beta peptide neurotoxicity in Alzheimer's disease. Nature 382 (6593), 685–691. https://doi.org/10.1038/382685a0.
Yin, L., Duan, J.J., Bian, X.W., et al., 2020. Triple-negative breast cancer molecular subtyping and treatment progress. Breast Cancer Res. 22 (1), 61. https://doi.org/10.1186/s13058-020-01296-5.
Zhang, H., Sun, S.C., 2015. NF-κB in inflammation and renal diseases. Cell Biosci. 5, 63. https://doi.org/10.1186/s13578-015-0056-4.